J Eng Math (2010) 68:165–178
DOI 10.1007/s10665-010-9372-1

Axisymmetric oscillations of a cupola-shaped shell

Ivan Gavrilyuk · Martin Hermann · Volodymyr Trotsenko · Yuriy Trotsenko · Alexander Timokha

Received: 2 June 2009 / Accepted: 12 April 2010 / Published online: 29 April 2010
© Springer Science+Business Media B.V. 2010

Abstract A spectral boundary problem on axisymmetric eigenoscillations of a cupola-shaped shell is considered with emphasis on small shell thickness. The problem deals with a singularly perturbed system of ordinary differential equations. The paper examines analytical properties of the solution and, based on that, constructs an appropriate functional basis for Ritz' method. Employing this basis provides fast convergence in the C^3-metrics.

Keywords Axisymmetric eigenoscillations · Boundary-layer behavior · Ritz method · Thin-walled cupola-shaped shell

1 Introduction

There is a wide range of analytical and numerical methods which can be successfully applied to solve the problem of forced and eigenoscillations of thin-walled shells. Examples partly related to our presentation are given by Anderson [1], Göller [2], Mukherjee and Chakraborty [3], and Al-Jumaily and Najim [4]. Anderson [1] considers the forced torsional oscillations of thin, spherical and hemispherical shells by using the Gegenbauer transform. Göller [2], and Mukherjee and Chakraborty [3] construct analytical solutions. Göller [2] employs the Flügge shell equations and uses modal superposition to get results for dynamic deformations of a spherical shell zone due to short-time local loads. The results are relevant to a nuclear boiling-water reactor. Results by Mukherjee and Chakraborty [3] are for thin neo-Hookean spherical shells. Al-Jumaily and Najim [4] present numerical and experimental results on axisymmetric free vibrations of a closed thin oblate spheroidal shell. The methods are useful, but it is difficult

I. Gavrilyuk
Berufsakademie Eisenach-Staatliche Studienakademie Thüringen, University of Cooperative Education, Am Wartenberg 2, 99817 Eisenach, Germany

M. Hermann
Friedrich-Schiller-Universität Jena, Ernst-Abbe-Platz 1-2, 07745 Jena, Germany

V. Trotsenko · Y. Trotsenko
Institute of Mathematics, National Academy of Sciences of Ukraine, Tereschenkivska 3 str., Kiev 01601, Ukraine

A. Timokha (✉)
CeSOS, Norwegian University of Science and Technology, 7091 Trondheim, Norway
e-mail: alexander.timokha@ntnu.no

to extend them to the analytical and numerical studies of the axisymmetric eigenoscillations of a cupola-shaped closed shell of revolution, i.e., to the tasks which are the focus of the present paper.

The eigenoscillations of the aforementioned axisymmetric shell are governed by a spectral boundary-value problem formulated for a system of ordinary differential equations (ODEs) which, to the authors best knowledge, do not have exact solutions. Appropriate approximate methods are reviewed in the book by Leissa [5, Chaps. 2, 6] as well as in books of Soviet applied mathematicians, e.g., Grigorenko et al. [6, Chap. 2], Karmishin et al. [7, Chap. 3] and Goldenveiser et al. [8, Chap. 8]. Because expressions for moments involve the third-order derivative of the eigenmodes, the approximate methods should, ideally, provide convergence in the C^3-metrics, namely, it should converge uniformly together with the third-order derivative. Whereas values of the shell thickness are not small, that is, *intermediate (moderate)*, the required approximation could, for instance, be achieved by reducing the original boundary-value problem to a recurrence of Cauchy problems that are integrated by the fourth-order Runge–Kutta method utilizing Godunov's discrete orthogonalization [8, pp. 124–126]. However, this method fails for thin-walled shells.

An alternative could be finite-element or Ritz' methods. A general finite-element method to compute eigenfrequencies and modes for ultimate shells of revolution is developed by Tan [9]. Vibrational behavior of a circular cylindrical shell, an elliptic hyperboloid shell (modeling a cooling tower), and a complete spherical shell are investigated by using this method. However, the applicability of this method is demonstrated for intermediate thickness, and, it is believed, the method needs special modifications to be adopted for the studied problem. Another example is in the paper by Sai Ram and Sreedhar Babu [10] who applied the finite-element method to a composite spherical shell as well as Panda and Singh [11] using the finite-element method for the geometrically large-amplitude free-vibration analysis of a composite spherical shell panel. Intermediate values of the shell thickness are studied in the papers by Kang and Leissa [12–16] who apply Ritz' method to two-dimensional and three-dimensional shell theory. Ritz' method and penalty parameters are used by Monterrubio [17] for a wide set of shells. We should mention the paper by Artioli et al. [18] who consider a free-vibration problem of shells of revolution and study the asymptotic behavior of the lowest eigenfrequency as the thickness tends to zero. The method is generally applicable to thin-walled shells. Numerical results are given by using a combination of finite-element and collocation methods for a parabolic, elliptic or a hyperbolic cylinder and a non-closed shell of revolution in the form of a dome-shaped shell with a hole at the top. It would be of great interest to illustrate how our method captures the asymptotics established by Artioli et al. [18], but, unfortunately, this paper does not give results for closed cupola-shaped shells that are studied here.

The reason for the limitation of numerical methods in handling thin-walled cupola-type shells of revolution is that the governing ODEs have a small multiplicative parameter (proportional to the thickness) in front of the highest-order derivative. As matter of the fact, the ODEs are singularly perturbed and their solution, that is, eigenmodes, is characterized by a boundary-layer behavior [19, Chap. 10] at the end-points of the considered interval. Analytical study of this behavior as well as an approximate numerical method providing a sufficient approximation in the C^3-metrics for both small and intermediate values of the shell thickness (the so-called uniformly converging method with respect to the thickness, [20, pp. 50–54]), were a challenge for the authors before writing this paper.

There are *two objectives* of the present paper. First, we investigate the character of the fundamental solution, and explicitly extract the boundary-layer-type component of this solution. Second, based on a variational formulation, a global Ritz method is applied using Legendre polynomials together with the boundary-layer solution. The constructed analytical approximate solutions are quite accurate to give an insight into the physics; they may also serve as a benchmark solution for traditional numerical tools.

In Sect. 2, the original boundary-value problem on axisymmetric eigenoscillations of the cupola-shaped shell (cutoffs of spheres, ellipsoids and hyperboloids of revolution are particular cases) is formulated and, in Sect. 3, the analytical structure of the eigenmodes is studied. The study makes it possible to construct a system of coordinate functions for Ritz' method (Ritz' method was used by Kang and Leissa [12–16], and Trotsenko [21], for a non-closed axisymmetric shell) which captures the boundary-layer behavior of the eigenmodes at the edge. In Sects. 4–6, the corresponding variational scheme involves these coordinate functions for numerical experiments demonstrating a

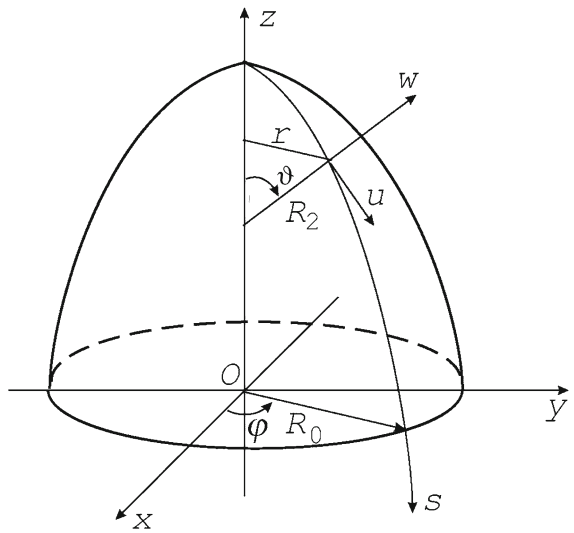

Fig. 1 Sketch of the cupola-shaped shell and adopted nomenclature. The axisymmetric shell eigenoscillations are associated with normal u and vertical tangential w shell displacements; the horizontal tangential displacement is zero.

good accuracy in the C^3 metrics. This accuracy is not affected by the shell thickness, i.e., the proposed method provides uniform convergence with respect to the thickness.

2 Statement of the problem

We consider an axisymmetric thin-walled shell of thickness h, whose mid-surface has a cupola-type shape in its static undeformed state as depicted in Fig. 1; R_0 is the shell characteristic dimension associated with the edge radius. The shell shape is fully determined by the meridional plane curve appearing due to intersection of the meridional plane and the mid-surface. This curve can be parameterized by the natural parameter s so that the starting point ($s = 0$) corresponds to the cupola pole and the end point ($s_1 > 0$) is at the shell edge, $0 \leqslant s \leqslant s_1$; obviously, s_1 is the total length of the curve.

Our focus is on *axisymmetric eigenoscillations* of the cupola-shaped shell. These oscillations are associated with small deviations of the introduced meridional plane curve so that the vertical tangential and normal (directed into the cupola) components, $U(s,t)$ and $W(s,t)$, respectively, are functions of s and t. The horizontal tangential component is zero. Because we consider eigenoscillations, $U(s,t) = \exp(\mathrm{i}\omega t)u(s)$ and $W(s,t) = \exp(\mathrm{i}\omega t)w(s)$, where the non-trivial functions $u(s)$ and $w(s)$ correspond to the eigenmodes, and ω is the circular eigenfrequency.

Following Aslanin and Lidski [22, Chap. 1], we consider nondimensional ordinary differential equations (ODEs) that describe axisymmetric eigenoscillations of the cupola-shaped shell and adopt the following notations

$$\Delta = \frac{1}{r}\frac{\mathrm{d}}{\mathrm{d}s}\left(r\frac{\mathrm{d}}{\mathrm{d}s}\right), \quad c^2 = \frac{h^2}{12R_0^2}, \quad \lambda = \frac{(1-\nu^2)\rho R_0^2\omega^2}{E},$$

where E, ν, ρ are Young' modulus, Poisson's coefficient and density, respectively. The *spectral parameter* λ is proportional to the square of the unknown eigenfrequency ω. The spectral ODEs with respect to the small deviations $u(s)$, $w(s)$ and λ take the form

$$\begin{aligned}
&-\frac{\mathrm{d}}{\mathrm{d}s}\left(\frac{1}{r}\frac{\mathrm{d}}{\mathrm{d}s}(ru)\right) - \frac{(1-\nu)}{R_1R_2}u + \frac{(1-\nu)}{R_2}\frac{\mathrm{d}w}{\mathrm{d}s} - \frac{\mathrm{d}}{\mathrm{d}s}\left(\left(\frac{1}{R_1}+\frac{1}{R_2}\right)w\right) - \lambda u = 0,\\
&\frac{1}{r}\left(\frac{1}{R_1}+\frac{1}{R_2}\right)\frac{\mathrm{d}}{\mathrm{d}s}(ru) - \frac{(1-\nu)}{r}\frac{\mathrm{d}}{\mathrm{d}s}\left(\frac{r}{R_2}u\right) + \left(\frac{1}{R_1^2}+\frac{2\nu}{R_1R_2}+\frac{1}{R_2^2}\right)w \qquad (1)\\
&\quad + c^2\left[\Delta\Delta w + \frac{(1-\nu)}{r}\frac{\mathrm{d}}{\mathrm{d}s}\left(\frac{r}{R_1R_2}\frac{\mathrm{d}w}{\mathrm{d}s}\right)\right] - \lambda w = 0.
\end{aligned}$$

The ODEs involve the principal curvatures, R_1 and R_2, which are expressed as

$$R_1 = -\frac{\sqrt{1-(r')^2}}{r''}, \quad R_2 = \frac{r}{\sqrt{1-(r')^2}}, \tag{2}$$

where $r(s)$ is the *known* distance between the meridional plane curve and the symmetry axis; $r' = \mathrm{d}r/\mathrm{d}s, r'' = \mathrm{d}^2r/\mathrm{d}s^2$.

The spectral problem (2) with respect to u, w, and spectral parameter λ requires corresponding boundary conditions at $s = s_1$. In the case of the clamped-edge shell, these conditions are

$$u(s_1) = w(s_1) = \frac{\mathrm{d}w}{\mathrm{d}s}|_{s=s_1} = 0. \tag{3}$$

The free-edge conditions suggest

$$T_1 = \frac{\mathrm{d}u}{\mathrm{d}s} + \frac{w}{R_1} + \nu\left(\frac{r'}{r}u + \frac{w}{R_2}\right) = 0, \quad M_1 = -c^2\left(\frac{\mathrm{d}^2w}{\mathrm{d}s^2} + \nu\frac{r'}{r}\frac{\mathrm{d}w}{\mathrm{d}s}\right) = 0,$$
$$Q_1 = -c^2\left(\frac{\mathrm{d}}{\mathrm{d}s}\Delta w + \frac{1-\nu}{R_1R_2}\frac{\mathrm{d}w}{\mathrm{d}s}\right) = 0 \ \text{ at } \ s = s_1, \tag{4}$$

where T_1, M_1, and Q_1 are the meridional force and moment, and the transverse force on the mid-surface, respectively. Different boundary conditions at the shell edge can involve a linear combination of (3) and (4).

At the cupola pole, $s = 0$, the functions $u(s)$ and $w(s)$ should be finite together with their derivatives. Moreover, the axisymmetric shell cupola is characterized by equal principal curvatures at the pole, i.e.,

$$(R_1)_{s=0} = (R_2)_{s=0} = R = \text{const} \tag{5}$$

so that $r(s)$ is an analytical function at $s = 0$.

3 Analytical structure of the eigenmodes

3.1 Preliminaries

Because the *known* function $r(s)$ and principal curvatures R_1 and R_2 defined by (2) are analytical functions, they can formally be expressed in terms of Taylor series, i.e.,

$$r(s) = s\left(1 - \frac{1}{6R^2}s^2 + a_4s^4 + \cdots\right); \tag{6}$$

$$\begin{aligned}\tfrac{1}{R_1} &= \tfrac{1}{R}\left[1 + \left(\tfrac{1}{8R^2} - 15R^2a_4\right)s^2 + b_4s^4 + \cdots\right],\\ \tfrac{1}{R_2} &= \tfrac{1}{R}\left[1 + \left(\tfrac{1}{24R^2} - 5R^2a_4\right)s^2 + c_4s^4 + \cdots\right],\end{aligned} \tag{7}$$

where a_i, b_i and c_i are the corresponding coefficients. Substituting (6) and (7) in (2), one can see that, even though $u(s)$ and $w(s)$ must be finite at $s = 0$, there are degenerating coefficients in the front of the derivatives of $u(s)$ and $w(s)$ at $s = 0$. This point is important for constructing regular asymptotic solutions in Sect. 3.2.

The second important point is that the highest-order derivative of $w(s)$ (associated with the $\Delta\Delta w$-term) in (2) is multiplied by the nondimensional thickness c which is assumed to be a small parameter. As matter of the fact, the considered ODEs (2) are singularly perturbed; their fundamental solution includes a high-gradient (boundary-layer type) component which will be derived in Sect. 3.3.

In this section, we construct asymptotic solutions of (2) in terms of the small parameter μ defined as follows

$$\mu^4 = c^2. \tag{8}$$

According to the general theory of singularly perturbed differential equations [19, Chap. 10] and [23, Chap. 4], there are three aforementioned types of asymptotic solutions which are associated here with the indexes $\mathcal{J} = 1, 2$ and 3. The first type ($\mathcal{J} = 1$) implies a regular (analytical) asymptotic solution, but $\mathcal{J} = 2, 3$ correspond to the boundary-layer-type solutions.

3.2 Regular asymptotic solution, $\mathcal{J} = 1$

The regular asymptotic solution of (2) can be presented as follows

$$u(s) = \sum_{k=0}^{\infty} \mu^{4k} u_k(s), \quad w(s) = \sum_{k=0}^{\infty} \mu^{4k} w_k(s), \tag{9}$$

where u_k and w_k should be found by inserting (9) into (2) and matching the same powers of μ on both sides of the differential equations. This procedure yields recurrence ODEs with respect to $u_k(s)$ and $w_k(s)$, $k \geq 0$. Our task consists of studying the asymptotic solution behavior at $s = 0$ which is fully *determined by the zero-order approximation*.

The zero-order ODEs couple $u_0(s)$ and $w_0(s)$, i. e.,

$$\alpha_1 \frac{\mathrm{d}u_0}{\mathrm{d}s} + \alpha_2 u_0 + \alpha_3 w_0 = 0, \quad \gamma_1 \frac{\mathrm{d}w_0}{\mathrm{d}s} + \gamma_2 w_0 + \gamma_3 u_0 = 0, \tag{10}$$

where the s-dependent coefficients are

$$\begin{aligned}
&\alpha_1 = \frac{1}{R_1} + \frac{\nu}{R_2}, \ \alpha_2 = \frac{r'}{r}\left(\frac{\nu}{R_1} + \frac{1}{R_2}\right), \ \alpha_3 = \frac{1}{R_1^2} + \frac{2\nu}{R_1 R_2} + \frac{1}{R_2^2} - \lambda, \\
&\gamma_2 = (1-\nu^2)\left[\frac{1}{R_1^2}\left(\frac{1}{R_2} - \frac{1}{R_1}\right)' + \frac{2}{R_1 R_2}\left(\frac{1}{R_2}\right)'\right] + \lambda\left[\left(\frac{1}{R_1}\right)' + (2\nu - 1)\left(\frac{1}{R_2}\right)'\right], \\
&\gamma_3 = (\nu - 1)\left(\frac{r'}{r}\right)'\left(\frac{1}{R_1^2} + \frac{\nu - 1}{R_1 R_2} - \frac{\nu}{R_2^2}\right) + (\nu^2 - 1)\frac{r'}{r}\left[\frac{1}{R_2}\left(\frac{1}{R_1}\right)' - \frac{1}{R_1}\left(\frac{1}{R_2}\right)'\right] \\
&\qquad + (1-\nu)\left(\frac{r'}{r}\right)^2\left(\frac{\nu}{R_1^2} - \frac{1}{R_2^2} + \frac{1-\nu}{R_1 R_2}\right) - \alpha_1^2\left(\lambda + \frac{1-\nu}{R_1 R_2}\right), \\
&\gamma_1 = -\alpha_1\left(\lambda - \frac{1-\nu^2}{R_2^2}\right).
\end{aligned} \tag{11}$$

Due to relations (6) and (7), the coefficients α_2 and γ_3 have a first-order pole, but other coefficients in (11) are analytical functions at $s = 0$. Physically, Eq. 10 describes eigenoscillations of a membrane shell.

Introducing the vector-function

$$\mathbf{y} = \{y_1, y_2\}, \quad y_1 = u_0(s), \quad y_2 = w_0(s), \tag{12}$$

the ODEs (10) can be re-written in the normal form

$$s\frac{\mathrm{d}\mathbf{y}}{\mathrm{d}s} = F(s, \lambda)\mathbf{y}, \tag{13}$$

where the elements $f_{ij}(s)$ of matrix $F(s, \lambda)$ are defined by

$$f_{11}(s) = -\frac{s\alpha_2(s)}{\alpha_1(s)}, \quad f_{12}(s) = -\frac{s\alpha_3(s)}{\alpha_1(s)}, \quad f_{21}(s) = -\frac{s\gamma_3(s)}{\gamma_1(s)}, \quad f_{22}(s) = -\frac{s\gamma_2(s)}{\gamma_1(s)}. \tag{14}$$

The functions $f_{ij}(s)$ are analytical on the interval $[0, s_1]$, and, therefore, we can present matrix $F(s, \lambda)$ in the Taylor series

$$F(s, \lambda) = \sum_{k=0}^{\infty} F_k s^k, \tag{15}$$

where the matrix coefficients F_k are given by

$$F_0 = \begin{Vmatrix} -1 & 0 \\ 0 & 0 \end{Vmatrix}, \ F_{2k-1} = \begin{Vmatrix} 0 & f_{12}^{(2k-1)} \\ f_{21}^{(2k-1)} & 0 \end{Vmatrix}, \ F_{2k} = \begin{Vmatrix} f_{11}^{(2k)} & 0 \\ 0 & f_{22}^{(2k)} \end{Vmatrix}, \quad (k = 1, \ldots).$$

The solution of the ODEs (13) can be expressed as

$$y_i = s^\sigma \sum_{k=0}^{\infty} g_{i,k} s^k, \quad (i = 1, 2), \tag{16}$$

where σ and $g_{i,k}$ are unknowns. The right-hand side of (13) is composed of the expressions

$$f_{pq} y_q = s^\sigma \sum_{k=0}^{\infty} \sum_{j=0}^{k} g_{q,j} f_{pq}^{(k-j)} s^k, \quad (p, q = 1, 2). \tag{17}$$

Substituting (16)–(17) in (13) and matching the terms of the lowest-order power of s leads to the spectral matrix problem

$$(F_0 - \sigma E)\mathbf{g}_0 = 0, \tag{18}$$

where E is the identity matrix and $\mathbf{g}_0 = (g_{1,0}, g_{2,0})$. The solvability condition $\det(F_0 - \sigma E) = 0$ gives the following two-solutions set

$$\sigma_1 = 0 \quad \text{with} \quad g_{1,0} = C, \ g_{2,0} = 0, \quad \text{and} \quad \sigma_2 = -1 \quad \text{with} \quad g_{1,0} = 0, \ g_{2,0} = C, \tag{19}$$

where C is an arbitrary constant. Furthermore, collecting coefficients in front of $s^{\sigma+k}$ $(k = 1, 2, \ldots)$ leads to the recurrent sequence of the *inhomogeneous* algebraic systems

$$[F_0 - (\sigma + k)]\mathbf{g}_k = \mathbf{d}_k, \quad d_i^{(k)} = -\sum_{q=1}^{2} \sum_{j=0}^{k-1} g_{q,j} f_{iq}^{(k-j)}, \tag{20}$$

where $\mathbf{g}_k$ is a vector with components $(g_{1,k}, g_{2,k})$.

Whereas $\sigma = \sigma_1 = 0$ (in (19)), solution (16) is analytic and takes the form

$$y_1(s) = u(s) = \sum_{k=1}^{\infty} g_{1,2k-1} s^{2k-1}, \quad y_2(s) = w(s) = \sum_{k=0}^{\infty} g_{2,2k} s^{2k}. \tag{21}$$

In contrast, the second root $\sigma = \sigma_2 = -1$ yields a physically irrelevant solution which tends to infinity as $s \to 0$.

The first-type solution (21) ($\mathcal{J} = 1$) depends only on the single arbitrary constant C. This dependence does not make it possible to satisfy three boundary conditions of (3) (or, alternatively, (4)). We need therefore two additional linearly independent solutions of the original ODEs.

3.3 Two boundary-layer asymptotic solutions, $\mathcal{J} = 2, 3$

According to the general theory of singularly perturbed ODEs (see, [19, Chap. 10], [23, Chap. 4]), the boundary-layer solution takes the form

$$u(s) = \mu\gamma(s) \sum_{k=1}^{\infty} \mu^k \tilde{u}_k(s), \quad w(s) = \gamma(s) \sum_{k=1}^{\infty} \mu^k \tilde{w}_k(s), \quad \gamma(s) = \exp\left\{ \frac{1}{\mu} \int_{s_0}^{s} \varphi(t) \mathrm{d}t \right\}, \tag{22}$$

where $0 < s_0 \le s_1$. The unknown functions $\varphi(s)$, $\tilde{u}_k(s)$ and $\tilde{w}_k(s)$ can be found by substituting expressions (22) in (2) and by matching the same powers of μ. The lowest-order approximation gives the following equation with respect to $\varphi(s)$

$$(\varphi(s))^4 - b_0(s) = 0, \quad b_0(s) = \lambda - \frac{1 - \nu^2}{R_2^2}. \tag{23}$$

Henceforth, we assume that $b_0(s) \neq 0$ and $b_0(s) < 0$ for $s \in [0, s_1]$. The second condition (negativeness of b_0) means that only a lower part of the spectrum is considered (λ is relatively small). Under this condition, the first

equation of (23) possesses the following two pairs of complex conjugate roots (ordered by increasing their real parts):

$$\varphi_1(s) = \frac{-1+\mathrm{i}}{\sqrt{2}}|b_0|^{1/4},\ \varphi_2(s) = \frac{-1-\mathrm{i}}{\sqrt{2}}|b_0|^{1/4},$$
$$\varphi_3(s) = \frac{1+\mathrm{i}}{\sqrt{2}}|b_0|^{1/4},\ \varphi_4(s) = \frac{1-\mathrm{i}}{\sqrt{2}}|b_0|^{1/4}. \tag{24}$$

Each of $\varphi_k(s), k = 1, ..., 4$ yields the corresponding particular solution of the original ODEs. Substituting $\varphi_k(s)$ with negative real parts in (22) leads to solutions which rapidly increase with decreasing s. These solutions are physically irrelevant for cupola-shaped shells, and thus we focus on φ_3 and φ_4.

When $s_0 = s_1$ in representation (22), substituting $\varphi_k(s), k = 3, 4$ in the original ODEs gives, after separation of real and imaginary parts, the multiplier $\gamma(s)$ which equals

$$\mathrm{e}^{\beta(s)}\cos\beta(s) \quad \text{or} \quad \mathrm{e}^{\beta(s)}\sin\beta(s), \quad \text{where} \quad \beta(s) = \frac{1}{\mu\sqrt{2}}\int_{s_1}^{s}|b_0(t)|^{1/4}\mathrm{d}t. \tag{25}$$

This multiplier is a strongly oscillating function for small values of μ, and it rapidly decays for $s < s_1$ away from the point s_1. This expresses the so-called *boundary-layer behavior* at the shell edge. Using multiplier γ and expressions by Tovstik [24] given for the ultimate ODEs, one can find functions $\tilde{u}_k(s)$ and $\tilde{w}_k(s)$ appearing in expressions (22).

The functions $\tilde{u}_k(s)$ and $\tilde{w}_k(s)$ can also be presented in Taylor series as $s \approx s_1$. This means that the two needed linearly independent solutions (in addition to the first-type solution (21)) read as follows:

$$u^{(\mathcal{J})}(s) = \mu\gamma^{(\mathcal{J})}(s)\sum_{k=0}^{\infty}\mu^k\left\{\sum_{i=0}^{\infty}u_{k,i}^{(\mathcal{J})}(s-s_1)^i\right\},$$
$$w^{(\mathcal{J})}(s) = \gamma^{(\mathcal{J})}(s)\sum_{k=0}^{\infty}\mu^k\left\{\sum_{i=0}^{\infty}w_{k,i}^{(\mathcal{J})}(s-s_1)^i\right\}, \quad (\mathcal{J} = 2, 3), \tag{26}$$

where $u_{k,i}^{(\mathcal{J})}$, $w_{k,i}^{(\mathcal{J})}$ are unknown coefficients, and

$$\gamma^{(\mathcal{J})}(s) = \begin{cases} \mathrm{e}^{\beta(s)}\cos\left(\beta(s)\right), & \mathcal{J} = 2, \\ \mathrm{e}^{\beta(s)}\sin\left(\beta(s)\right), & \mathcal{J} = 3. \end{cases}$$

Even though $\beta(s)$ is not expressed in elementary functions, solution (26) can, as shown by Vishik and Lusternik [23, Chap. 4], be presented in the asymptotic form

$$\left[u^{(\mathcal{J})}(s), w^{(\mathcal{J})}(s)\right] = \exp\{\varphi_{\mathcal{J}+1}(s_1)\tau\}\sum_{k=0}^{\infty}\mu^k P_{\mathcal{J}}^{(k)}(\tau), \quad \mathcal{J} = 2, 3, \tag{27}$$

where $\tau = (s - s_1)/\mu$, and $P_{\mathcal{J}}^{(k)}(\tau)$ are polynomials in τ of the order $2k$ with constant coefficients depending on coefficients of (2) and their derivatives at $s = s_1$.

3.4 General structure of the fundamental solution

In *summary*, accounting for three linearly independent solutions, (21) and (26), whose linear combination makes it possible to satisfy the boundary conditions at the edge, the eigenmodes $[u, w]$ admit the fundamental solution

$$[u, w] = R[u, w] + \mathrm{e}^{\beta(s)}\cos\beta(s)\sum_{i=0}^{\infty}[u_{i,1}, w_{i,1}](s-s_1)^i + \mathrm{e}^{\beta(s)}\sin\beta(s)\sum_{i=0}^{\infty}[u_{i,2}, w_{i,2}](s-s_1)^i, \tag{28}$$

where $R[u, w]$ is a regular analytic component (presented, e.g., by (21)), $\beta(s)$ is given by (23) and (25), and $u_{i,1}$, $u_{i,2}$ and $w_{i,1}$, $w_{i,2}$ are unknown constants (including the parameter μ) which will be found after substitution of (28) in the original ODEs and boundary conditions.

4 Variational formulation

An appropriate variational formulation follows from the principle of virtual displacements which can be written in the form

$$\delta A = \delta \Pi, \tag{29}$$

where $\delta\Pi$ is the variation of the potential energy (work done by the body forces), and δA is the external virtual work associated with the inertia forces. In a nondimensional statement [25, pp. 47–48], the potential energy Π and the virtual work δA (free oscillations of the shell) are expressed as

$$\Pi = \tfrac{1}{2}\int_0^{s_1}\left[\varepsilon_1^2+\varepsilon_2^2+2\nu\varepsilon_1\varepsilon_2+c^2(\kappa_1^2+\kappa_2^2+2\nu\kappa_1\kappa_2)\right]r\,\mathrm{d}s,\quad \delta A=\lambda\int_0^{s_1}(u\delta u+w\delta w)r\,\mathrm{d}s,$$

where the mid-surface deformations are given by the formulas

$$\varepsilon_1=\frac{\mathrm{d}u}{\mathrm{d}s}+\frac{w}{R_1},\quad \varepsilon_2=\frac{r'}{r}u+\frac{w}{R_2},\quad \kappa_1=-\frac{\mathrm{d}^2w}{\mathrm{d}s^2},\quad \kappa_2=-\frac{r'}{r}\frac{\mathrm{d}w}{\mathrm{d}s}.$$

The variational equation (29) for the considered problem then takes the form

$$\int_0^{s_1}[\Psi_{11}(u,\delta u)+\Psi_{12}(w,\delta u)+\Psi_{12}(\delta w,u)+\Psi_{22}(w,\delta w)]r\,\mathrm{d}s-\lambda\int_0^{s_1}(u\delta u+w\delta w)r\,\mathrm{d}s=0, \tag{30}$$

where (p and q are general substitutes for real and test functions)

$$\Psi_{11}(\mathrm{p},\mathrm{q})=\left(\frac{\mathrm{dp}}{\mathrm{d}s}+\frac{\nu r'}{r}\mathrm{p}\right)\frac{\mathrm{dq}}{\mathrm{d}s}+\left[\nu\frac{r'}{r}\frac{\mathrm{dp}}{\mathrm{ds}}+\left(\frac{r'}{r}\right)^2\mathrm{p}\right]\mathrm{q},$$

$$\Psi_{12}(\mathrm{p},\mathrm{q})=\left(\frac{1}{R_1}+\frac{\nu}{R_2}\right)\mathrm{p}\frac{\mathrm{dq}}{\mathrm{d}s}+\frac{r'}{r}\left(\frac{1}{R_2}+\frac{\nu}{R_1}\right)\mathrm{pq},$$

$$\Psi_{22}(\mathrm{p},\mathrm{q})=\left(\frac{1}{R_1^2}+\frac{2\nu}{R_1R_2}+\frac{1}{R_2^2}\right)\mathrm{pq}+c^2\left\{\frac{\mathrm{d}^2\mathrm{p}}{\mathrm{d}s^2}\frac{\mathrm{d}^2\mathrm{q}}{\mathrm{d}s^2}+\left[\frac{\nu r'}{r}\frac{\mathrm{d}^2\mathrm{p}}{\mathrm{d}s^2}+\left(\frac{r'}{r}\right)^2\frac{\mathrm{dp}}{\mathrm{d}s}\right]\frac{\mathrm{dq}}{\mathrm{d}s}+\frac{\nu r'}{r}\frac{\mathrm{dp}}{\mathrm{d}s}\frac{\mathrm{d}^2\mathrm{q}}{\mathrm{d}s^2}\right\}.$$

One should note that the dynamic boundary conditions, here free-edge conditions (4), are natural, namely, following from variational equation (30), but the clamped-end conditions (3) are not natural, the trial functions should *a priory* satisfy the clamped-end conditions, if stated.

5 Global Ritz' method

We employ variational equation (30) and Ritz' method (with coordinate functions to be consistent with fundamental solution (28)) to solve spectral problem (2) with boundary conditions (3). The functions $u(s)$ and $w(s)$ are presented in the form

$$u(s)=\sum_{j=1}^{N}x_jU_j(s),\quad w(s)=\sum_{j=1}^{N}x_{j+N}W_j(s), \tag{31}$$

where x_j $(j=1,2,\ldots,2N)$ are unknown constants and $\{U_j(s)\}$ and $\{W_j(s)\}$ are coordinate functions that satisfy the clamped-end boundary conditions.

Substitution of (31) in the variational equation (30) yields the matrix spectral problem

$$(A-\lambda B)\mathbf{x}=0,\quad \mathbf{x}=(x_1,x_2,\ldots,x_{2N}) \tag{32}$$

with symmetric matrices A and B. To get this spectral matrix problem, we pose $\delta u = U_i(s)$ and $\delta w = 0$ in (30) for the first N equations of (32), but $\delta u = 0$ and $\delta w = W_i(s)$ leads to the remaining N equations. Elements $\{a_{ij}\} = A$ and $\{b_{ij}\} = B$ are

$$a_{i,j} = \int_0^{s_1} \Psi_{11}(U_j, U_i) r \mathrm{d}s, \quad a_{i+N,j+N} = \int_0^{s_1} \Psi_{22}(W_j, W_i) r \mathrm{d}s,$$

$$b_{i,j} = \int_0^{s_1} U_j, U_i r \mathrm{d}s, \quad b_{i+N,j+N} = \int_0^{s_1} W_j, W_i r \mathrm{d}s, \quad (i = 1, 2, \ldots, N;\ j \geqslant i),$$

$$a_{i,j+N} = \int_0^{s_1} \Psi_{12}(W_j, U_i) r \mathrm{d}s, \quad b_{i,j+N} = 0, \quad (i, j = 1, 2, \ldots, N).$$

According to (28), the coordinate functions have the following structure

$$\begin{aligned} \{U_i(s)\}_{i=1}^N &= \{U_1, \ldots, U_m; U_{m+1}, \ldots, U_{m+m_p}; U_{m+m_p+1}, \ldots, U_{m+2m_p}\}, \\ \{W_i(s)\}_{i=1}^N &= \{W_1, \ldots, W_m; W_{m+1}, \ldots, W_{m+m_p}; W_{m+m_p+1}, \ldots, W_{m+2m_p}\}, \end{aligned} \tag{33}$$

where the first group (consisting of m regular functions) involve the Legendre polynomials, $P_j(\cdot)$, modified to satisfy the clamped-end conditions, but the second and third group (each of m_p functions) are associated with the $\mathrm{e}^\beta \cos\beta$- and $\mathrm{e}^\beta \sin\beta$-quantities from (28), respectively. Explicit expressions for the coordinate functions $U_j(s)$ and $W_j(s)$ take the form

$$\begin{aligned} U_j &= s\left(s^2 - s_1^2\right) P_{2j-1}\left(\frac{2s}{s_1} - 1\right), \\ W_j &= \left(s^2 - s_1^2\right)^2 P_{2j-1}\left(\frac{2s}{s_1} - 1\right), \quad (j = 1, 2, \ldots, m), \\ U_{m+1} &= g_c - \frac{s}{s_1}, \quad U_{m+2} = (s - s_1) g_c, \quad U_{m+m_p+1} = g_s, \quad U_{m+m_p+2} = (s - s_1) g_s, \\ W_{m+1} &= g_c - 1 - \frac{p}{2s_1}\left(s^2 - s_1^2\right), \quad W_{m+2} = (s - s_1) g_c - \frac{1}{2s_1}\left(s^2 - s_1^2\right), \\ W_{m+m_p+1} &= g_s - \frac{p}{2s_1}\left(s^2 - s_1^2\right), \quad W_{m+m_p+2} = (s - s_1) g_s, \\ U_{m+k} &= W_{m+k} = (s - s_1)^{k-1} g_c, \\ U_{m+m_p+k} &= W_{m+m_p+k} = (s - s_1)^{k-1} g_s, \quad (k = 3, 4, \ldots, m_p). \end{aligned} \tag{34}$$

Here, the functions $g_c(s)$ and $g_s(s)$ are

$$\begin{aligned} g_c &= \exp\{p_\mu(s - s_1)\} \cos(p_\mu(s - s_1)), \quad g_s = \exp\{p_\mu(s - s_1)\} \sin(p_\mu(s - s_1)), \\ p_\mu &= p_\mu(\lambda) = \frac{\sqrt[4]{\left|\lambda - \frac{1-\nu^2}{R_2^2(s_1)}\right|}}{\left(\mu\sqrt{2}\right)}. \end{aligned} \tag{35}$$

Computations of the Legendre polynomials and their first- and second-order derivatives can be performed by using the recursive relations

$$\begin{aligned} P_{j+2}(s) &= \frac{1}{j+1}\left[(2j+1) s P_{j+1}(s) - j P_j(s)\right], \\ P'_{j+2}(s) &= s P'_{j+1}(s) + (j+1) P_{j+1}(s), \quad P''_{j+2}(s) = s P''_{j+1}(s) + (j+2) P'_{j+1}(s), \\ P_1(s) &= 1, \quad P_2(s) = s, \quad P_3(s) = \tfrac{1}{2}(3s^2 - 1). \end{aligned}$$

Table 1 Convergence to the five lowest eigenfrequencies versus the number of regular coordinate functions

m	ω_1	ω_2	ω_3	ω_4	ω_5
$\delta = 100$					
2	0.424822	0.810329	0.935994	1.036195	1.595648
4	0.424767	0.801161	0.886484	0.925515	1.091895
6	0.424767	0.801159	0.885994	0.920509	0.951959
8	0.424767	0.801159	0.885994	0.920490	0.943053
10	0.424767	0.801159	0.885994	0.920490	0.942929
12	0.424767	0.801159	0.885994	0.920490	0.942929
$\delta = 1000$					
2	0.407475	0.810061	0.962506	1.067890	1.541983
4	0.407312	0.791919	0.880269	0.925323	0.959443
6	0.407312	0.791908	0.878332	0.910762	0.929201
8	0.407312	0.791908	0.878330	0.910476	0.925902
10	0.407312	0.791908	0.878330	0.910476	0.925853
12	0.407312	0.791908	0.878330	0.910476	0.925853
$\delta = 2000$					
2	0.405188	0.810334	0.966930	1.070927	1.562291
4	0.404998	0.790777	0.879828	0.926367	0.960434
6	0.404998	0.790765	0.877607	0.910297	0.929309
8	0.404998	0.790765	0.877605	0.909941	0.925456
10	0.404998	0.790765	0.877605	0.909941	0.925388
12	0.404998	0.790765	0.877605	0.909941	0.925388

The number of the boundary-layer coordinate functions is restricted to 2, i.e., $m_p = 2$. A spherical-cap shell with $\vartheta_f = 135°$ is considered

An important fact is that parameter p_μ in (35) depends on λ and, therefore, problem (32) is, generally speaking, nonlinear with respect to λ. An approximation of the eigenvalues can be computed by using only a regular basis, that is, with $m_p = 0$ in (33). One can employ this approximation as an initial approximation in an iterative procedure which uses $\lambda^{(k)}$ from the previous step in expression for p_μ in (35) to get the next approximation $\lambda^{(k+1)}$ from the linear spectral problem (32). Numerical experiments establish a fast convergence of this iterative procedure so that only two or three steps are needed to stabilize six to seven significant figures of the lower eigenvalues.

6 Numerical results

Convergence of the constructed Ritz method and features of the eigenmodes are illustrated for a spherical-cap shell with a clamped edge. The characteristic dimension R_0 is the shell edge radius; $\delta = R_0/h$. The angle between the symmetry axis and the normal vector to the mid-surface is ϑ (see, Fig. 1), which is equal to ϑ_f along the clamped-edge curve. Numerical experiments are performed with the Poisson coefficient equal to 0.3.

Table 1 presents approximate nondimensional lower eigenfrequencies, $\omega_i = \sqrt{\lambda_i}$, $i = 1, ..., 5$, for three values of δ versus the number of regular coordinate functions; $\vartheta_f = 135°$; two coordinate functions possessing the boundary-layer behavior are used, that is, $m_p = 2$. The table demonstrates a fast convergence so that six significant figures are provided by $m = 10$ for both small and intermediate shell thickness. Our numerical experiments establish analogous convergence for other physical and geometric parameters of the tested spherical-shape shells.

An advantage of the method is that it provides uniform convergence (for both small and intermediate shell thickness) to deflections, meridional force T_1 and moment M_1, and transverse force Q_1. This is even though

Table 2 Convergence to the values of w, T_1, M_1 and Q_1 for the first eigenmode $[u_1, w_1]$ at $\vartheta^* = \vartheta/\vartheta_f = 0.95$ versus the number of regular coordinate functions

m	w_1	T_1	M_1	Q_1
$\delta = 100$				
2	−0.48655	0.32695	-0.3572×10^{-3}	0.1540×10^{-2}
4	−0.47964	0.32650	-0.3433×10^{-3}	0.1330×10^{-2}
6	−0.47954	0.32654	-0.3427×10^{-3}	0.1332×10^{-2}
8	−0.47953	0.32654	-0.3427×10^{-3}	0.1333×10^{-2}
10	−0.47952	0.32653	-0.3427×10^{-3}	0.1333×10^{-2}
12	−0.47952	0.32653	-0.3427×10^{-3}	0.1333×10^{-2}
$\delta = 1000$				
2	−0.66267	0.30698	0.2381×10^{-5}	0.1218×10^{-4}
4	−0.66974	0.31265	0.1276×10^{-5}	-0.1936×10^{-4}
6	−0.66974	0.31285	0.1253×10^{-5}	-0.2058×10^{-4}
8	−0.66972	0.31286	0.1253×10^{-5}	-0.2078×10^{-4}
10	−0.66971	0.31286	0.1254×10^{-5}	-0.2085×10^{-4}
12	−0.66970	0.31286	0.1256×10^{-5}	-0.2085×10^{-4}
14	−0.66970	0.31286	0.1256×10^{-5}	-0.2084×10^{-4}
$\delta = 2000$				
2	−0.65883	0.30248	0.7736×10^{-8}	0.1982×10^{-4}
4	−0.66188	0.31066	0.6321×10^{-7}	0.1384×10^{-4}
6	−0.66158	0.31068	0.6789×10^{-7}	0.1371×10^{-4}
8	−0.66154	0.31067	0.6874×10^{-7}	0.1372×10^{-4}
10	−0.66153	0.31067	0.6908×10^{-7}	0.1374×10^{-4}
12	−0.66153	0.31067	0.6913×10^{-7}	0.1375×10^{-4}
14	−0.66153	0.31067	0.6901×10^{-7}	0.1376×10^{-4}

The number of the boundary-layer-type coordinate functions in (33) is $m_p = 2$. A spherical-cap shell with $\vartheta_f = 135°$ is considered. The numerical eigenmodes are normalized to get maximum shell bending in the direction of the outer normal equal to one

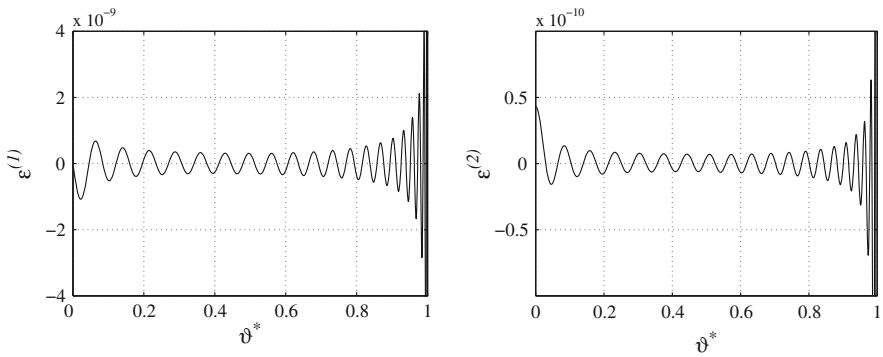

Fig. 2 Error-estimates $\varepsilon^{(i)}(\vartheta^*)$ with $\delta = R_0/h = 2000$ and $\vartheta_f = 90°$. Hemispherical shell

computations of T_1, M_1, and Q_1 need up to the third-order derivative of the corresponding eigenmode. Table 2 illustrates convergence for the same spherical-cap shell as in Table 1 at a point close to the shell edge. One can see that this convergence to normal deflection of the first eigenmode, w_1 as well as to T_1, M_1, and Q_1 is fast.

An error estimate of the constructed uniformly converging method (for the first eigenmode) may be demonstrated by the functions $\varepsilon^{(i)} = \varepsilon^{(i)}(\vartheta^*)$, $\vartheta^* = \vartheta/\vartheta_f \in [0, 1]$ $(i = 1, 2)$ which imply errors in satisfying the governing ODEs (2). The errors are computed by substitution of the Ritz solution in expressions (2). Figure 2 shows $\varepsilon^{(i)}(\vartheta^*)$ for a thin hemispherical shell with a clamped edge; $\vartheta_f = 90°$ and $\delta = R_0/h = 2000$. As we have already mentioned,

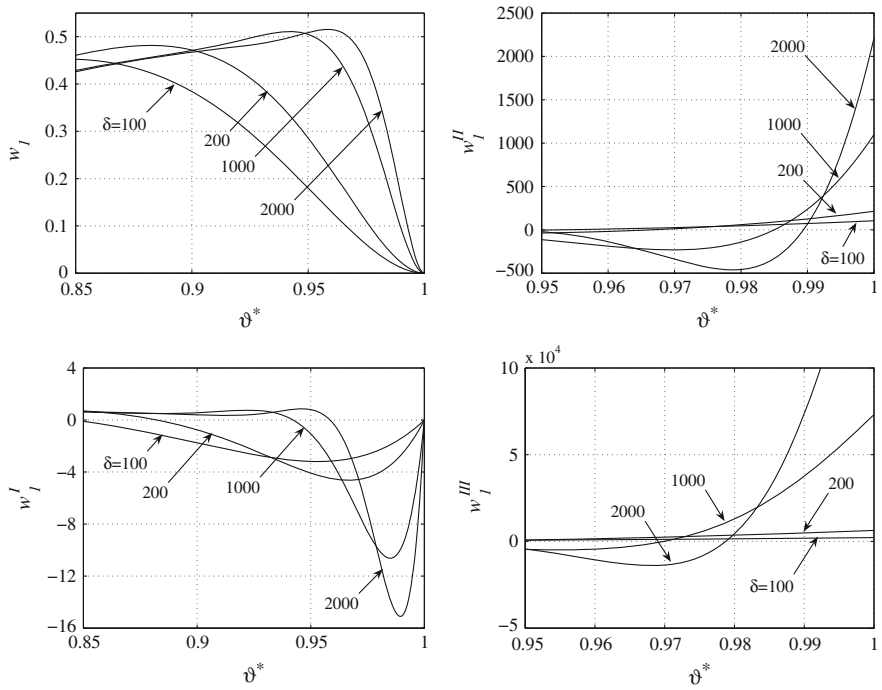

Fig. 3 Normal deflection $w_1(\vartheta^*)$ (first eigenmode) and their derivatives, $w_1^I = w_1'$, $w_1^{II} = w_1''$ and $w_1^{III} = w_1'''$, in a neighborhood of the edge for different values of $\delta = R_0/h$. Hemispherical shell

the largest error occurs in the vicinity of the clamped boundary. However, this error remains small for the whole interval, namely, for $\vartheta^* \in [0, 1]$.

The normal deflection $w(\vartheta^*)$ and its derivatives in the vicinity of the clamped edge (the first eigenmode, $[u_1, w_1]$) are shown in Fig. 3 for a hemispherical shell and different values of $\delta = R_0/h$. The figure exhibits a boundary-layer behavior of these functions when the thickness becomes smaller (with increasing δ). This means that a purely regular functional basis does not provide fast convergence for small shell thickness and the coordinate functions governed by (26) are strongly needed to get a satisfactory approximation in the C^3-metrics.

Figure 4 demonstrates the boundary-layer behavior of $T_1(\vartheta^*)$, $M_1(\vartheta^*)$ and $Q_1(\vartheta^*)$ for different values of ϑ_f and $\delta = R_0/h = 150$. This value of δ implies an intermediate thickness; however, one can see that $T_1(\vartheta^*)$, $M_1(\vartheta^*)$ and $Q_1(\vartheta^*)$ (excluding T_1 for $\vartheta_f = 90°$) demonstrate a rapid change in a neighborhood of the clamped edge. This means that, even though using the boundary-layer coordinate functions is not necessary for getting satisfactory approximation of the eigenfrequencies and modes, these functions are required for the associated force and moment.

7 Concluding remarks and discussion

Regular and boundary-layer behavior at clamped edges has been described analytically for axisymmetric eigenmodes of a thin-walled cupola-shaped shell of revolution. Capturing the boundary-layer behavior is necessary for coordinate functions of Ritz' method to provide uniform convergence to the eigenmodes, to get accurate approximation of the associated force and moment. This has been illustrated for spherical-cap shells, but the authors have established similar results for other axisymmetric shell shapes.

Another important point is that the governing ODEs have degenerating coefficients in front of the higher derivatives at the shell pole, but the eigenmodes should remain regular. The presence of these degenerating coefficients is a problem for many numerical schemes. To avoid this problem, Kang and Leissa [13], Medvedev and Sokov [26]

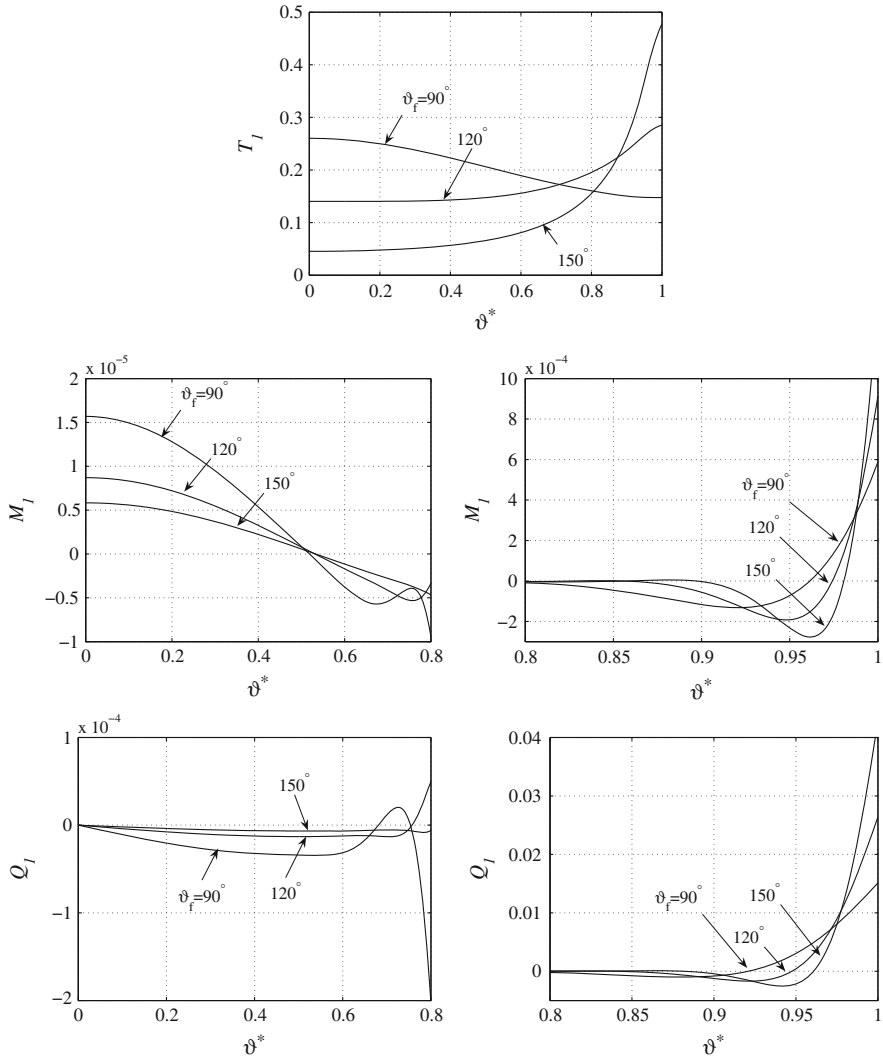

Fig. 4 Force T_1 and moment M_1, and transverse force Q_1 for different values ϑ_f and $\delta = R_0/h = 150$. Hemispherical shell

and some other authors *postulate* the presence of a small circular hole at the cupola pole attributed by the free-edge boundary conditions:

$$(T_1)_{\vartheta=\vartheta_0} = (M_1)_{\vartheta=\vartheta_0} = (Q_1)_{\vartheta=\vartheta_0} = 0 \tag{36}$$

at this artificial hole edge. Physically, assuming this artificial hole means that the cupola-shaped shell without the hole behaves similar to the shell with a small hole at the pole. Mathematically, this means that our numerical solution must be close to those constructed in the aforementioned papers.

Our numerical experiments showed that the eigenfrequencies from the paper by Medvedev and Sokov [26] are indeed close to those obtained by our numerical method. The same holds true for the transverse force Q_1. Figure 4 demonstrates that Q_1 tends to zero when $s \to 0$. However, the figure illustrates the fact that T_1 and M_1 are not zero at the pole; they tend to finite non-zero values as $\vartheta_0 \to 0$. This means that the first and second conditions of (36) are, generally, not fulfilled for the limit eigenmodes without small hole. In summary, assuming the artificial hole with the free-edge conditions (36) may be adopted for computing the eigenfrequencies, but this is not applicable if the task consists of getting meridional force and moment.

Acknowledgement Authors thank the German Research Society (DFG) for financial support (project DFG 436UKR 113/33/03).

References

1. Anderson GL (1970) On Gegenbauer transforms and forced torsional vibrations of thin spherical shells. J Sound Vib 12:265–275
2. Göller B (1980) Dynamic deformations of thin spherical shells based on analytical solutions. J Sound Vib 73:585–596
3. Mukherjee K, Chakraborty SK (1985) Exact solution for larger amplitude free and forced oscillation of a thin spherical shell. J Sound Vib 100:339–342
4. Al-Jumaily AM, Najim FM (1997) An approximation to the vibrations of oblate spheroidal shells. J Sound Vib 207:561–574
5. Leissa AW (1993) Vibration of shells. The Acoustical Society of America, New York
6. Grigorenko YaM, Bespalova EI, Kitaigorodski AB, Shinkar AI (1986) Eigen oscillations of elements of shell-like constructions. Naukova Dumka, Kiev (in Russian)
7. Karmishin AV, Lyaskovets VA, Myachenkov VI, Frolov AN (1975) Statics and dynamics of thin-walled constructions. Mashinostroenie, Moscow (in Russian)
8. Goldveiser AL, Lidski VB, Tovstic PE (1979) Eigen oscillations of thin elastic shells. Nauka, Moscow (in Russian)
9. Tan D-Y (1998) Free vibration analysis of shells of revolution. J Sound Vib 213:15–33
10. Sai Ram KS, Sreedhar Babu T (2002) Free vibration of composite spherical shell cap with and without a cutout. Comput Struct 80:1749–1756
11. Panda SK, Singh BN (2009) Nonlinear free vibration of spherical shell panel using higher order shear deformation theory—a finite element approach. Int J Press Vessels Piping 86:373–383
12. Kang JH, Leissa AW (2000) Three-dimensional vibrations of thick spherical shell segments with variable thickness. Int J Solids Struct 37:4811–4823
13. Kang JH, Leissa AW (2004) Three-dimensional vibration analysis of thick, complete conical shells. Trans ASME 71:502–507
14. Kang JH, Leissa AW (2005) Three-dimensional vibration analysis of thick hyperboloidal shells of revolution. J Sound Vib 282:277–296
15. Kang JH, Leissa AW (2005) Free vibration analysis of complete paraboloidal shells of revolution with variable thickness and solid paraboloids from a three-dimensional theory. Comput Struct 83:2594–2608
16. Kang JH, Leissa AW (2008) Vibration analysis of solid ellipsoids and hollow ellipsoidal shells of revolution with variable thickness from a three-dimensional theory. Acta Mechanica 197:97–117
17. Monterrubio IE (2009) Free vibration of shallow shells using the Rayleigh–Ritz method and penalty parameters. Proc IMechE C 223:2263–2272
18. Artioli E, Beiraoda Veiga L, Hakula H, Lovadina C (2009) On the asymptotic behaviour of shells of revolution in free vibration. Comput Mech 44:45–60
19. Wasow W (2002) Asymptotic expansions for ordinary differential equations. Courier Dover Publications
20. Doolan EP, Miller JJH, Schilders WHA (1980) Uniform numerical methods for problems with initial and boundary layers. Boole Press, Dublin
21. Trotsenko VA, Trotsenko YuV (2005) Solution of the problem on eigen oscillations of a non-closed shell of revolution under conditions of singular perturbations. Nonlinear Oscil 8:415–432
22. Aslanyan AG, Lidski VB (1974) Distribution of eigen frequencies of thin elastic shells. Nauka, Moscow (in Russian)
23. Vishik MI, Lusternik LA (1957) Regular degeneracy and boundary layer for linear differential equations with a small parameter. Uspekhi Math Nauk 12(5(77)):3–122
24. Tovstik PE (1975) Low-frequency oscillations of a convex shell of revolution. Izvestiya AN SSSR, Mechanics of solid body no. 6, pp 110–116 (in Russian)
25. Novozhilov VV (1962) Theory of thin shells. Sudostroenie, Leningrad (in Russian)
26. Medvedev VI, Sokov LM (1975) On eigenoscillations of spherical shells. Appl Probl Saf Plast (2):36–43 (in Russian)